

See discussions, stats, and author profiles for this publication at: <https://www.researchgate.net/publication/12382152>

Improved Calibration of Time-of-Flight Mass Spectra by Simplex Optimization of Electrostatic Ion Calculations

ARTICLE *in* ANALYTICAL CHEMISTRY · AUGUST 2000

Impact Factor: 5.64 · DOI: 10.1021/ac991500h · Source: PubMed

CITATIONS

14

READS

15

3 AUTHORS, INCLUDING:



Randy J Arnold

AB SCIEX

56 PUBLICATIONS 1,535 CITATIONS

SEE PROFILE

Improved Calibration of Time-of-Flight Mass Spectra by Simplex Optimization of Electrostatic Ion Calculations

Noah P. Christian,[†] Randy J. Arnold,[‡] and James P. Reilly*

Department of Chemistry, Indiana University, Bloomington, Indiana 47405

A novel time-of-flight mass calibration method has been developed. In contrast to conventional methods, where the relationship between ion flight time and mass is an arbitrary polynomial equation, this method is based on the physics of ion motion. Parameters needed to describe the physics are numerically optimized using a simplex algorithm. Once these parameters are established, unknown masses can be determined from their times-of-flight. This calibration method gives intrinsically well-behaved results, since nonlinearities (due to extraction delay, desorption velocity, etc.) are properly taken into account in the time-of-flight calculation. The simplex method is compared to curve fitting for the analysis of time-of-flight data, and some significant advantages are demonstrated. Salient features of the method include greatly improved mass extrapolation accuracy, no loss of interpolated calibration accuracy, the ability to obtain an accurate calibration with a minimal number of calibrants, and the ability to extract unknown parameters such as desorption velocities.

Matrix-assisted laser desorption (MALDI)¹ and electrospray ionization (ESI)² have dramatically facilitated mass spectrometric analysis of synthetic and biological macromolecules. These methods are largely responsible for a resurgence of interest in time-of-flight (TOF) mass spectrometry. Advantages of time-of-flight mass analyzers include an unlimited mass range and the ability to analyze all ions extracted at one time. The TOF analyzer is sensitive to initial spatial, velocity, and temporal distributions,³ and considerable effort has been devoted to improving its resolution and mass accuracy. Improving resolution aids in the ability to identify very small mass changes in large molecules, to distinguish molecular ions from adducts, and to sequence biopolymers. Resolution in a conventional MALDI-TOF instrument is primarily limited by velocity distributions of source ions. The

greatest improvement in MALDI-TOF resolution has come from pulsed ion extraction, which was demonstrated first by the groups of Reilly,⁴ Brown,⁵ and Li⁶ and subsequently by that of Vestal.⁷ The use of pulsed electric fields overcomes some of the limitations induced by the initial-velocity distribution.^{4–7} An ESI-TOF instrument typically incorporates an orthogonal source to minimize these initial-velocity effects.⁸

In an idealized time-of-flight instrument, an ion with zero initial velocity has a time-of-flight equal to a constant times the square root of its mass. Curve fits using this simplified relationship are easy to perform, and this is a well-established technique.⁹ The initial velocity of MALDI ions negates the validity of this simple expression.^{10–12} Vestal and Juhasz have discussed the exact form of the time-of-flight relationship while taking into account initial-ion-velocity components for a number of instrument configurations.¹² Unfortunately, an expression for the mass-to-charge ratio in terms of flight time cannot be derived in closed form. Some approximation is therefore necessary for curve-fit calibrations. It has been noted that mass calibration of spectra with a linear time-of-flight instrument improves with the use of a three-term mass fit.¹⁰ Juhasz et al.¹¹ proposed a modified three-term equation that

[†] Present address: Centre National de Genotypage, 2 rue Gaston Cremieux, CP 5721, 91057 Evry Cedex, France.

[‡] Present address: Department of Chemistry, Huntingdon College, 1500 E. Fairview Lane, Montgomery, AL 36106.

- (1) Karas, M.; Bachmann, D.; Bahr, U.; Hillenkamp, F. Matrix-Assisted Ultraviolet Laser Desorption of Nonvolatile Compounds. *Int. J. Mass Spectrom. Ion Processes* **1987**, *78*, 53–68.
- (2) Fenn, J. B.; Mann, M.; Meng, C. K.; Wong, S. F.; Whitehouse, C. M. Electrospray Ionization for Mass Spectrometry of Large Molecules. *Science* **1989**, *246*, 64–71.
- (3) Opsal, R. B.; Owens, K. G.; Reilly, J. P. Resolution in the Linear Time-of-Flight Mass Spectrometer. *Anal. Chem.* **1985**, *57*, 1884–1889.

- (4) Colby, S. M.; King, T. B.; Reilly, J. P. Improving the Resolution of Matrix-Assisted Laser Desorption/Ionization Time-of-Flight Mass Spectrometry by Exploiting the Correlation between Ion Position and Velocity. *Rapid Commun. Mass Spectrom.* **1994**, *8*, 865–868.
- (5) Brown, R. S.; Lennon, J. J. Mass Resolution Improvement by Incorporation of Pulsed Ion Extraction in a Matrix-Assisted Laser Desorption/Ionization Linear Time-of-Flight Mass Spectrometer. *Anal. Chem.* **1995**, *67*, 1998–2003.
- (6) Whittall, R. M.; Li, L. High-Resolution Matrix-Assisted Laser Desorption/Ionization in a Linear Time-of-Flight Mass Spectrometer. *Anal. Chem.* **1995**, *67*, 1950–1954.
- (7) Vestal, M. L.; Juhasz, P.; Martin, S. A. Delayed Extraction Matrix-Assisted Laser Desorption Time-of-Flight Mass Spectrometry. *Rapid Commun. Mass Spectrom.* **1995**, *9*, 1044–1050.
- (8) Chernushevich, I. V.; Ens, W.; Standing, K. G. Orthogonal-Injection TOFMS for Analyzing Biomolecules. *Anal. Chem.* **1999**, *71*, 452A–461A.
- (9) Cotter, R. J. *Time-of-Flight Mass Spectrometry*; ACS Symposium Series 549; American Chemical Society: Washington, DC, 1994; p 17 ff.
- (10) Vera, C. C.; Zubarev, R.; Ehring, H.; Hakansson, P.; Sunqvist, B. U. R. A Three-Point Calibration Procedure for Matrix-Assisted Laser Desorption/Ionization Mass Spectrometry Utilizing Multiply Charged Ions and Their Mean Initial Velocities. *Rapid Commun. Mass Spectrom.* **1996**, *10*, 1429–1432.
- (11) Juhasz, P.; Vestal, M. L.; Martin, S. A. On the Initial Velocity of Ions Generated by Matrix-Assisted Laser Desorption Ionization and Its Effect on the Calibration of Delayed Extraction Time-of-Flight Mass Spectra. *J. Am. Soc. Mass Spectrom.* **1997**, *8*, 209–217.
- (12) Vestal, M.; Juhasz, P. Resolution and Mass Accuracy in Matrix-Assisted Laser Desorption Ionization-Time-of-Flight. *J. Am. Soc. Mass Spectrom.* **1998**, *9*, 892–911.

includes desorption velocity and extraction delay terms. Their method allows one to extract unknown initial desorption velocities.

Despite the need for approximations in curve-fit calibrations, MALDI-TOF instrumentation can exhibit impressive performance. Whittall and Li demonstrated mass accuracies of 7 ppm (parts per million).⁶ Using a long flight tube (4.2 m) and reflectron (0.9 m), Edmonson and Russell obtained better than 3 ppm accuracy.¹³ Brown and Lennon even demonstrated 100 ppm accuracy for ions formed by in-source fragmentation.¹⁴

Using an expression that closely models the behavior of an ion in electric fields, Panitz et al. demonstrated an alternative method for calibrating a field-desorption TOF mass spectrometer.¹⁵ They noted that two factors limited their ability to relate theoretical calculations to actual times-of-flight: the pulse delay and the ion formation time in the source. These uncertainties could be corrected with a least-squares optimization. Parameters were adjusted until the calculations for known masses matched actual times-of-flight in the instrument. Following this optimization, unknown masses could be calculated using measured times-of-flight.

The calculation of optimized pulsed ion extraction fields in a MALDI-TOF instrument for improving resolution has been previously discussed.¹⁶ Because these electrostatic calculations contain information relating ion masses and flight times, they would be useful for mass calibration if the instrument conditions were precisely defined. Unfortunately, because of errors in the measurement of distances and voltages and the penetration of fields from one region into another, this is not the case. High voltages are particularly difficult to accurately measure, especially when these involve very rapidly time-varying potentials. Moreover, all of the instrument parameters are subject to drift. Their large number makes it difficult to refine them using a nonlinear least-squares optimization. The system can easily be underdetermined, since there may be many more instrument parameters than available mass calibrants. This problem can be overcome if the calculations are optimized with a simplex routine. Simplex algorithms are useful for the optimization of systems that are underdetermined or whose measurements are obscured by experimental error. These algorithms are very efficient when a large number of parameters require optimization.¹⁷ Simplex algorithms may also fit functions that cannot be analytically expressed.^{18,19}

In the current work, we present a novel approach to calibrating TOF mass spectra that uses simplex-optimized instrumental operating parameters in elementary ion physics calculations. The method starts with a description of the instrument that includes all distances, delay times, voltages, and ion parameters such as initial velocity and position. Most of these instrument parameters may be measured with reasonable accuracy. A computer algorithm uses this description to compute flight times for different ion masses. Using a set of calibration points, these parameters are refined using simplex optimization. The result is that these numerically optimized parameters now provide a computationally accurate description of the instrument. Using optimized parameters, any mass may be directly input to calculate the expected time-of-flight. The inverse of this calculation—transforming times-of-flight to masses—completes the calibration procedure. Because the method does not use an analytical expression, complex boundary conditions such as time-varying electric fields are easily managed.²⁰

The present paper describes this calibration algorithm and demonstrates the use of the method. A comparison with conventional curve fitting is drawn, and advantages and disadvantages of each method are explored.

EXPERIMENTAL SECTION

Algorithm Development. The simplex engine was adapted from the *amoeba* algorithm contained in Numerical Recipes.²¹ This algorithm was based on the Nelder–Mead simplex algorithm.¹⁹ The minimization used in this algorithm involved computing residual errors between an array of experimental flight times and calculated flight times. The algorithm reiteratively optimized the instrument parameters to minimize the difference between experimental and calculated flight times. Any residual error function can be used in the minimization routine. Variations show differing performances in terms of convergence speed and accuracy. For all calculations contained in this paper, the sum of the squares of differences between experimental and calculated flight times was used.

Two of the input parameters needed by the simplex algorithm were the λ value and the fit tolerance. The λ value is the characteristic length vector used to define the initial simplex dimensions in the optimization routine. In general, we matched vector components to measurement uncertainties. For example, static voltages were given a 25 V λ value because this was the estimated measurement error anticipated in an actual system, whereas pulse voltages were given a 250 V λ value. These numbers can be reduced or increased, depending on anticipated measurement accuracies and drifts. Excessively small values needlessly increased computational time. The fit tolerance represents the desired conditions for termination of the optimization and is based on the expected error between experimental and optimized calculations. As with the λ value, a value that was too small greatly increased iterative requirements of the calculation. An excessively large number caused the simplex navigation to terminate before a minimum was found.

- (13) Edmonson, R. D.; Russell, D. H. Evaluation of Matrix-Assisted Laser Desorption Ionization Time-of-Flight Mass Measurement Accuracy by Using Delayed Extraction. *J. Am. Soc. Mass Spectrom.* **1996**, *7*, 995–1001.
- (14) Brown, R. S.; Lennon, J. J. Sequence-Specific Fragmentation of MALDI Protein/Peptide Ions. *Anal. Chem.* **1995**, *67*, 3990–3999.
- (15) (a) Panitz, J. A. The Crystallographic Distribution of Field-Desorbed Species. *J. Vac. Sci. Technol.* **1974**, *11*, 206–210. (b) Panitz, J. A.; McLane, S. B.; Müller, E. W. The Atom-Probe Field Ion Microscope. *Rev. Sci. Instrum.* **1968**, *39*, 83–86. (c) Panitz, J. A. *A Simplified Calibration Sequence for Single-Atom Mass Spectrometers*; NTIS Report SAND75-0116; NTIS: Springfield, VA, 1975; 16 pp. (d) Panitz, J. A.; McLane, S. B.; Müller, E. W. Calibration of the Atom Probe FIM. *Rev. Sci. Instrum.* **1969**, *40*, 1321–1324.
- (16) Colby, S. M.; Reilly, J. P. Space-Velocity Correlation Focusing. *Anal. Chem.* **1996**, *68*, 1419–1428.
- (17) Spendley, W.; Hext, G. R.; Himsworth, F. R. Sequential Aspects of Simplex Designs in Optimisation and Evolutionary Operation. *Technometrics* **1962**, *4*, 441–461.
- (18) Powell, M. J. D. An efficient Method for Finding the Minimum of a Function of Several Variables without Calculating Derivatives. *Computer J.* **1965**, *7*, 155–162.
- (19) Nelder, J. A.; Mead, R. A Simplex Method for Function Minimization. *Computer J.* **1965**, *7*, 308–313.

- (20) Christian, N. P.; Arnold, R. J.; Reilly, J. P. *Proceedings of the 46th ASMS Conference*; 1998; p 126.
- (21) Press, W. H.; Teukolsky, S. A.; Vetterling, W. T.; Flannery, B. P. *Numerical Recipes in C: The Art of Scientific Computing*, 2nd ed; Cambridge University Press: New York, 1992.

For mass calibration by curve fitting, either SigmaPlot (SPSS, Chicago, IL) or a Marquardt–Levenberg algorithm²² using the code contained in Numerical Recipes²⁰ was used. When a TOF spectrum is converted to mass, peak areas must remain consistent. Because of the nonlinear relation between mass and TOF, two peaks occurring on a TOF axis with equal height and width will differ in aspect when plotted on a linear mass scale. The peak appearing earlier will have a higher intensity and a narrower width. Our curve-fitting software and the simplex software both accounted for these changes. For establishing peak locations, we employed a Gaussian centroid calculation that was also contained in our software.

Instruments and Sample Preparation. Two instruments were used for the experimental measurements. Both had a two-stage ion source with a subsequent drift region and are closely represented by previous descriptions.²³ All samples were desorbed using a frequency-tripled Nd:YAG laser at 355 nm.

A protein calibration sample was prepared by the following method: A 1 μ L mixture of approximately 10 mg/mL α -cyano-4-hydroxycinnamic acid (CHC), 150 ng/mL bradykinin, 25 μ g/mL ubiquitin, and 150 μ g/mL cytochrome *c* in a 70:30 mixture of 0.1% aqueous trifluoroacetic acid and acetonitrile was deposited on a stainless steel probe and allowed to air-dry.

An alkanethiolate-coated gold nanocrystal sample, described in previous work,²⁴ was dissolved in a minimal amount of toluene. One microliter of this solution was deposited on a stainless steel probe and allowed to air-dry.

A nucleic acid sample was prepared using a 0.5 μ L volume of 10 pmol/ μ L analyte with 1 μ L of a saturated 3-hydroxypicolinic acid solution in a 1:1 mixture of acetonitrile and water and 1 μ L of a 3 mmol/mL solution of diammonium citrate. The analyte sequence was TTTTATTTTT where all T's were deoxythymidines and A was a 2'-methoxyadenine.

RESULTS AND DISCUSSION

Curve-fitting and simplex optimization approaches were compared using both theoretical and experimental data. Since an operating instrument is limited in its ultimate accuracy, theoretical data can better demonstrate some of the tenets of the different calibration methods. To verify that these comparisons were valid for actual calibrations, we also examined lower precision experimental data.

Curve Fitting. Curve fitting can be used to determine unknown masses on the basis of ion times-of-flight. A typical TOF equation is

$$\text{TOF} = a(m/z)^{1/2} + b \quad \text{when } v_0 = 0 \quad (1)$$

where TOF is the time-of-flight of an ion, *a* and *b* are constants based upon instrument parameters, and *m/z* is the mass-to-charge

ratio of the ion. Alternatively the equation

$$m/z = a'(\text{TOF})^2 + b' \quad \text{when } v_0 = 0 \quad (2)$$

is often used. For conventional curve fitting, a function in the form of eq 2 is fit to a list of calibration points. The equation thus becomes the calibration curve for a range of ions.⁹

When the ion has an initial velocity and there is an extraction delay, the time-of-flight equation becomes considerably more complex. Given some assumption about the ion position at the time of the extraction pulse, a mathematically exact expression for TOF can nevertheless be derived for an instrument. This equation contains variables for distances, voltages, initial velocities, etc. and may appear relatively complicated. It can be expanded into an infinite series, which is helpful for several reasons. First, since the first term in the TOF expression is the only one that is nonzero when $x_0 = 0$ and $v_0 = 0$, it allows for comparison of higher order nonlinearities in time-of-flight behavior. Second, although the exact values for the coefficients change from one geometry to another, the form of the series does not. Thus, this expanded form of the equation is valid for any TOF instrument. Third, since we ultimately want to convert flight times to masses, this equation can be inverted to accomplish this. The Taylor expansion of a time-of-flight expression yields an infinite series:

$$\text{TOF} - k = a(m/z)^{1/2} + b(m/z) + c(m/z)^{3/2} + d(m/z)^{5/2} + e(m/z)^{7/2} + \dots \quad (3)$$

where *a*, *b*, *c*, ... are constants related to the instrument geometry and conditions and the constant *k* represents the inability to locate an exact start time of the ion extraction. This infinite series resembles multiple-term calibration equations,^{10,11} but the complete series is an exact expression of ion behavior. Understanding this infinite series is important for understanding curve-fit calibrations. Unfortunately, use of eq 3 for mass calibration is complicated by the fact that the variable of greatest interest, *m/z*, is not expressed as a function of the experimentally measured variable TOF. In fact, multiple values of *m/z* are associated with the same value of TOF. The series can be inverted to an equation that is much easier to use for calibration. This inversion allows the determination of a single mass, given a time-of-flight, and has the form

$$m/z = a'(\text{TOF} - k)^2 + b'(\text{TOF} - k)^3 + c'(\text{TOF} - k)^4 + d'(\text{TOF} - k)^5 + e'(\text{TOF} - k)^6 + \dots \quad (4)$$

The coefficients (*a'*, *b'*, *c'*, ...) in eq 4 are different from the constants (*a*, *b*, *c*, ...) in eq 3.

The infinite series of eqs 3 and 4 permit an exact description of an ion's time-of-flight in a delayed-extraction instrument. Although the use of a finite number of terms leads to approximate results, this is necessary for curve fitting. For example, to create a four-parameter fit, the equation would be

$$m/z = a'(\text{TOF} - k)^2 + b'(\text{TOF} - k)^3 + c'(\text{TOF} - k)^4 \quad (5)$$

While eq 5 appears to be a three-term equation, expanding

(22) Marquardt, D. W. An Algorithm for Least-Squares Estimation of Nonlinear Parameters. *J. Soc. Ind. Appl. Math.* **1963**, *11*, 431–441.

(23) Christian, N. P.; Colby, S. M.; Giver, L.; Houston, C. T.; Arnold, R. J.; Ellington, A. D.; Reilly, J. P. High-Resolution Matrix-Assisted Laser Desorption/Ionization Time-of-Flight Analysis of Single-Stranded DNA of 27 to 68 Nucleotides in Length. *Rapid Commun. Mass Spectrom.* **1995**, *9*, 1061–1066.

(24) Arnold, R. J.; Reilly, J. P. High-Resolution Time-of-Flight Mass Spectra of Alkanethiolate-Coated Gold Nanocrystals. *J. Am. Chem. Soc.* **1998**, *120*, 1528–1532.

Table 1. Instrument Parameters for Simulations

| | | | |
|----------------|-------|-------------------|-----|
| V_0 (V) | 5000 | d_1 (mm) | 6 |
| V_1 (V) | 5000 | d_2 (mm) | 12 |
| V_2 (V) | 0 | L (m) | 0.4 |
| V_3 (V) | 0 | d_3 (mm) | 12 |
| V_4 (V) | -1800 | d_4 (mm) | 6 |
| V_{\max} (V) | 2500 | τ (μ s) | 2.1 |
| v_0 (m/s) | 600 | | |

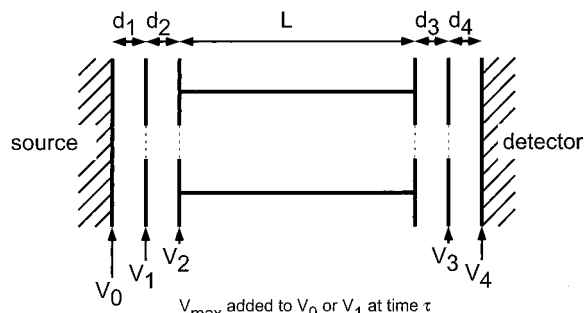


Figure 1. Schematic of the instrument geometry used in these discussions.

cross-terms leads to the expression

$$m/z = a'' + b'(\text{TOF}) + c'(\text{TOF})^2 + d'(\text{TOF})^3 + e''(\text{TOF})^4 \quad (6)$$

(The exact relationship between k , a' , b' , ... and a'' , b'' , ... can be algebraically determined.) The equation now appears to contain five terms. Evidently, cross-terms affect the apparent number of terms and parameters, so if we quantify these, we must be explicit in describing what equation is being discussed. In this work, we will refer to the eq 4 form that does not expand cross-terms. With theoretically generated calibration points, the constant k should be zero, so k is only included when experimental data or theoretical data having deliberately incorporated errors are fitted.

The effect of the number of terms in eq 4 on the quality of mass calibrations was investigated using theoretical data. To generate theoretically perfect data pairs of mass and time-of-flight, we defined instrument conditions (voltages, distances, etc.) that were used in time-of-flight calculations. Once these parameters were established, the time-of-flight associated with any mass value could be calculated to any desired precision. Each (m/z , TOF) pair was thus free of measurement error. We generated 101 points by this method to evaluate various methods of fitting data. The conditions for these calculations are listed in Table 1, and a schematic of the instrument is displayed in Figure 1. We then fit the 101 points using various equations that follow the form of eq 4 with the number of terms ranging from 2 to 5. Differences between masses generated by the TOF calculation and those predicted by the curve fit (the residual errors) were then calculated and are displayed in Figure 2A. The ordinate is highly expanded, showing very small errors in the overall fits. Increasing the number of terms evidently decreased the magnitude of the fit error and greatly increased the calibration accuracy. For example, accuracies improved by 6 orders of magnitude when the number of terms increased from 2 to 5. Instrument precision is rarely better than parts per million (ppm) in experiments, and

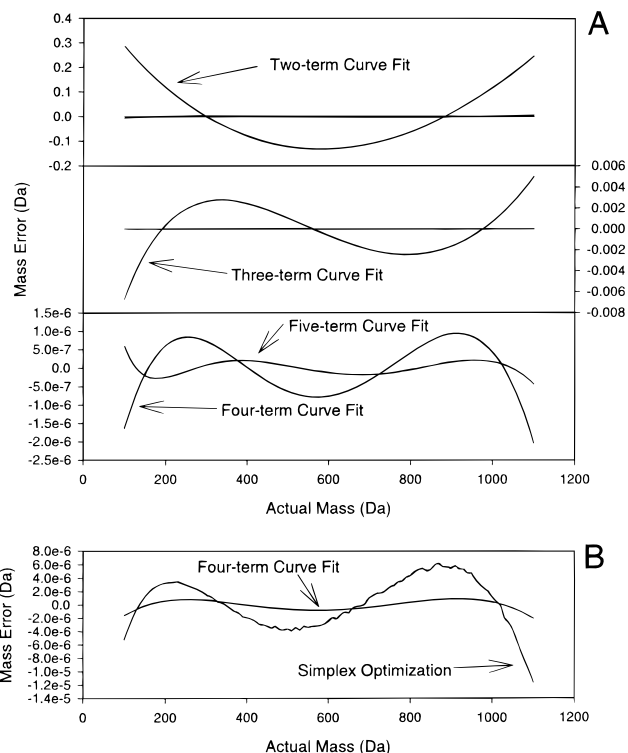


Figure 2. (A) Plots of residual errors in mass calibration by curve fitting using various numbers of terms. (B) Expanded-scale compression of simplex calibration and a four-term curve fit.

the accuracy of a fit cannot exceed instrumental limitations. Nevertheless, these theoretical calculations demonstrate that additional terms can be important for very accurate curve fitting. The number of terms used in an actual calibration is limited by the number of calibrants. For example, it would be impossible to solve for a five-term expansion if only two calibration points were available. As seen in Figure 2A, plot shapes are also affected by the number of terms. Curves cross zero once for each term in the equation. These error minima dictate the portion of the spectrum that has the smallest error. Although the data in Figure 2a are intended to show plot shapes and relative magnitudes of the curve-fit error, the absolute magnitude of the errors will vary with instrument geometry. As instrumental conditions approach those of d.c. ion extraction (short τ , small d_1 , large L), contributions from the additional higher order terms of eq 4 decrease and the best curve-fit calibration equation approaches the form of eq 2.

Simplex Optimization. The simplex optimization method is fundamentally different from curve fitting. For the simplex method, ion times-of-flight are calculated in each region of the instrument. This computation uses an exact electrostatic expression for ion motion with measured instrument parameters. Any difference between calculated and actual times-of-flight arises from errors in the measured instrument parameters used in the calculation. The process of optimization involves adjusting selected parameters so that theoretical and actual times-of-flight agree. The scheme for simplex optimization is shown in Figure 3. Starting with a list of calibrant masses and flight times, the simplex optimization adjusts parameters in the electrostatic TOF calculation to minimize errors between theoretical and calculated flight times. This gives a new list of optimized instrument parameters that can be used

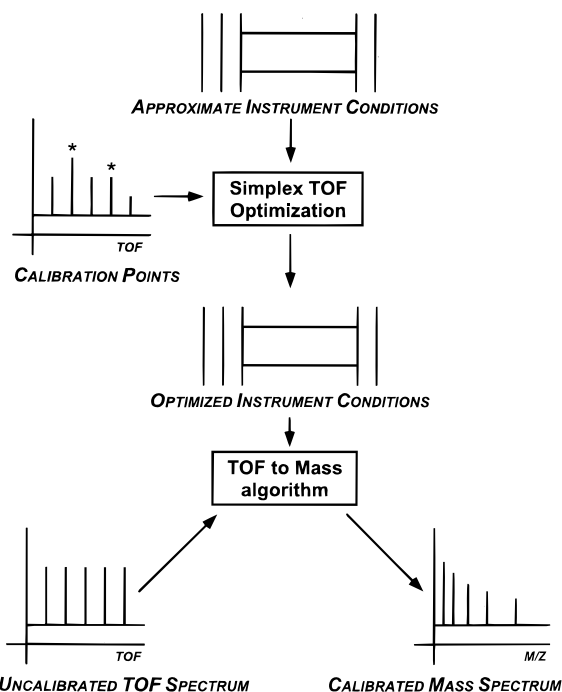


Figure 3. Overview of the simplex optimization method for mass calibration. Measured instrument conditions are adjusted using calibration points and a simplex/time-of-flight algorithm. These new conditions are then used to convert a time-of-flight spectrum to a mass spectrum. The necessary correction of peak heights when time-of-flight is converted to mass is also indicated.

to more accurately relate ion mass and TOF. After the corrected parameters are found, the reverse calculation of deriving mass from an observed TOF involves a simple numerical calculation.

To evaluate the algorithm's ability to calibrate masses, we performed test calibrations using the same 101-point theoretical data set discussed in the curve-fitting examples above. Since these data were generated using exactly known instrument parameters, we arbitrarily introduced errors in the initial values of the instrument parameters. This allowed us to test whether the simplex algorithm would converge on the proper values. Errors on the order of 10% of each parameter value were introduced. After optimization was performed on all parameters, the resulting residuals were plotted. Figure 2B demonstrates that simplex optimization yields a much lower residual error than a three-term curve fit and approaches the results of four- and five-term curve fits. Once again, experimental data have poorer accuracy than either calibration method at its ultimate performance level. Despite this, we will make some further theoretical comparisons before discussing experimental results.

Calibrating Data with Varied Levels of Determinism. The ability to calibrate masses over extended ranges would be advantageous, particularly if this could be accomplished with a minimal number of calibrants. It would be particularly useful if masses could be accurately determined outside the range of calibrants. To test this, additional simulated data were generated. The instrument geometry of Figure 1 and conditions listed in Table 1 were used. The electrostatic TOF calculation yielded flight times for $m/z = 100$, 101, and 110 Da, which were used as calibrants, and for $m/z = 5995.658$ Da, which was a test point. These values and their TOFs are summarized in Table 2. Calibrant

Table 2. Theoretical Calibration Points

| point | true mass (Da) | time-of-flight (μ s) |
|-------|----------------|---------------------------|
| 1 | 100.000 | 3.887 05 |
| 2 | 101.000 | 3.906 43 |
| 3 | 110.000 | 4.076 69 |
| extra | 5995.658 | 30.000 00 |

points are not normally chosen to be so far away from a mass of interest. Nevertheless, this extrapolation was a stringent test of how accurately each method modeled the relationship between TOF and mass. A curve fit to eq 2 resulted in a calibration equation that gave a calculated mass of 5958.619 Da for the 30.000 μ s test point (corresponding to a mass error of 37 Da). The error was due to the insufficiency of three calibration points and two terms in accurately describing the higher order terms of eq 4. When a four-term calibration equation was used, the calculated mass for the test point was 5977.929 Da, corresponding to an 18 Da mass error. The improvement from using additional terms is thus evident.

The simplex method can calibrate the extrapolated test point using the same data. As previously discussed, since theoretical data are generated using the same calculations and parameters as those for the simplex optimization, we needed to introduce an initial error in at least one parameter to test the optimization algorithm. A change in V_{\max} from 2500 to 100 V introduced a significant initial error. The simplex algorithm optimized this parameter to minimize errors in the calibration array, converging on the V_{\max} value of 2500.01 V. This yielded a calibrated value for the test point of 5995.649 Da which is in error by 0.009 Da (1.5 ppm). This accuracy could not be accomplished with a two-term curve fit.

Multiple unknown parameters are a much better test of this algorithm's performance. We investigated the effect of changing the V_{\max} value from 2500 to 100 V and τ from 2.1 to 2.8 μ s. The simplex algorithm (using the same calibrants) converged on $V_{\max} = 2437.128$ V and $\tau = 1.828$ μ s. Using these parameters, the error in the test point was 0.750 Da (126 ppm). Though the calibration was worse than the single-parameter case, it still performed much better than the curve fit.

The previous two examples were for an overdetermined system (three calibrants and one or two parameters). To evaluate a precisely determined system (equal number of calibrants and unknowns), V_{\max} , τ , and V_3 were changed from their initial values. The optimized parameters were $V_{\max} = 2437.15$ V, $\tau = 1.650$ μ s, and $V_3 = 1684.86$ V. The error in the test point was still only 0.750 Da (126 ppm). Thus with three calibrants, three unknown parameters may be optimized and still accurately model ion flight.

An underdetermined system—where there are more unknowns than calibrants—demonstrates the power of the simplex algorithm. V_{\max} , τ , V_3 , and d_3 were allowed to vary. Optimizing this system yielded $V_{\max} = 1115.09$ V, $\tau = 0.813$ μ s, $V_3 = 1105.09$ V, and $d_3 = 11.91$ mm. The resulting error in the test point was 0.545 Da (91.4 ppm). This demonstrated that the *underdetermined* simplex calibration was better than the *overdetermined* curve fit. Table 3 summarizes these results and demonstrates the improved results with the simplex calibration method for the test point. An analogous curve fit, where there are more variables to fit than

Table 3. Errors in Test Points for both Curve Fitting and Simplex Optimization

| calibration method | determinism | error at TOF = 30.000 μ s | |
|-------------------------|--------------------|-------------------------------|------|
| | | Da | ppm |
| two-term curve fit | overdetermined | 36.377 | 6100 |
| four-term curve fit | exactly determined | 18.11 | 3040 |
| one-parameter simplex | overdetermined | 0.009 | 1.5 |
| two-parameter simplex | overdetermined | 0.750 | 126 |
| three-parameter simplex | exactly determined | 0.750 | 126 |
| four-parameter simplex | underdetermined | 0.545 | 91.4 |

available calibration points, would be impossible to perform. Optimizing other parameters through the simplex procedure yielded similar results.

Instability Comparisons between Curve-Fit and Simplex Calibration. The previous comparison of the simplex method with curve fitting when extrapolated masses were considered was performed using theoretically perfect mass/TOF calibrants. Whether the method maintains accuracy and stability when the calibration points are not perfect is an issue that must be addressed. All samples are subject to measurement errors. In MALDI-TOF mass spectrometry, a calibrant mass can be misassigned or shifted in mass by an unanticipated factor (such as oxidation, loss of water, or adduction with alkali metals). A well-behaved function will not excessively degrade a calibration if a calibrant is misassigned. If the function is not well-behaved, inflection points will lead to unpredictable behavior, limiting the accuracy of extrapolating, or even interpolating, masses.

To demonstrate how simplex optimization maintains stability when calibration points are imperfect, we calculated flight times for masses of 100, 200, 300, and 400 Da using the conditions listed in Table 1. Calibrations were performed using curve fitting and simplex optimization with the 200 and 400 Da calibration points and misassigning the other two masses to 110 and 310 Da. Curve fitting predicted a mass of -39976 Da for the test point that should have a mass of 5995.658 Da. For simplex optimization, V_{\max} and L were optimized, resulting in $V_{\max} = 22420$ V and $L = 0.7647$ m. The obvious errors in V_{\max} and L are indicative of an error in the fit. Despite this, the new parameters predict a mass of 6077.80 Da, or an 82.2 Da error for the test point that should have mass of 5995.658 Da. Figure 4 illustrates the cause of this extreme error. The calibration points are exactly fit to the curve-fit equation, but since the calibrants are incorrect, the calibration curve diverges wildly outside this mass region. This introduces errors in both extrapolated and interpolated regions. In contrast, simplex optimization models the behavior of ions in electric fields and it yields a better behaved calibration curve.

Experimental Data. The performance advantages of simplex optimization demonstrated with the previous theoretical calculations are also evident in experimental studies performed with a MALDI-TOF instrument in our laboratory. An important difference in actual data is that the start time of the ion flight is subject to experimental error. Equation 4 includes a comparable parameter k . With simplex, more attention must be paid to this parameter, which we call the start-time error; because we are computing the flight times on the basis of instrument parameters, exact start times must be known. In these comparisons, all of the curve fits

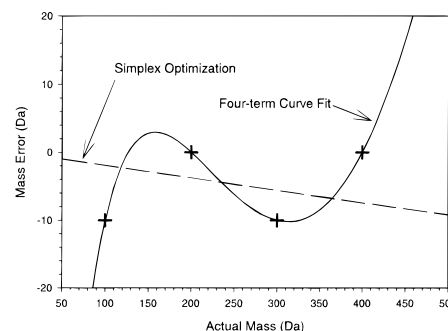


Figure 4. Time-of-flight errors as a function of mass using improperly assigned calibration points. Curve-fit calibration fits the calibration points (shown as crosshairs) with low residual error, at the expense of accuracy both inside and outside the calibration region.

Table 4. Measured Instrument Parameter Summaries

| | protein | DNA | gold |
|-------------------|---------------------|-------------------|-------------------|
| V_0 (V) | 20 000 | -15 000 | 20 000 |
| V_1 (V) | 20 000 | -15 000 | 20 000 |
| V_2 (V) | 0 | 0 | -1800 |
| V_3 (V) | 0 | 0 | -1800 |
| V_4 (V) | -1800 | -1900 | -1800 |
| V_{\max} (V) | -10 700 (G_1) | -3400 (G_0) | -5554 (G_1) |
| d_1 (mm) | 13.82 | 10.22 | 13.63 |
| d_2 (mm) | 19.74 | 13.96 | 27.51 |
| L (m) | 0.38098 | 0.11985 | 0.32111 |
| d_3 (mm) | 0 | 0 | 0.1 |
| d_4 (mm) | 3.54 | 9.71 | 12.79 |
| τ (μ s) | 0.5 | 2.0 | 3.3 |
| v_0 (m/s) | 600 | 600 | 600 |

follow the form of eq 4, where mass is expressed as a function of TOF. Measured instrument parameters are listed in Table 4. Any of these parameters can be chosen for optimization. In general, we found it best to select parameters that were subject to the greatest measurement error. We have also discovered through many trials that one or two parameters are usually sufficient to perform an accurate mass calibration. Performing an optimization and then selecting other parameters and reoptimizing does not improve the calibration. The first optimization changes parameters sufficiently that any reoptimization is not needed. Sometimes, however, parameters will be linked such that an optimization will not work. For example, if there is a d.c. accelerating voltage in the source that is optimized along with the desorption velocity, the algorithm will not usually be able to accurately estimate either the magnitude of the electric field or the desorption velocity. From trial and error, we have found a general list of parameters that work well as follows: V_{\max} , flight tube length, τ , start-time error, V_0 voltage (which is equal to V_1), and any other distance except for d_1 . The reason for eliminating d_1 from this list is that d_1 , V_{\max} , τ , and the start-time error are coupled parameters, and if simultaneously optimized, the algorithm converges on unreasonable values for them that do not improve the calibration accuracy. The optimization of several randomly selected sets of variables reflecting the freedom that one has in choosing parameters will be discussed.

A peptide mixture (bradykinin, ubiquitin, and cytochrome *c*) using a matrix of α -cyano-4-hydroxycinnamic acid served as the sample for a rather stringent comparison of the two calibration methods, since this represents a rather broad mass range. The

Table 5. Calibration Comparisons between Curve Fit and Simplex Optimization

| identity | known mass (amu) | measd TOF (ns) | calibrated masses (amu) ^a | |
|------------------------------------|------------------|----------------|--------------------------------------|------------------|
| | | | curve fit | simplex |
| [bradykinin + H] ⁺ | 1061.180 | 7483.074 | 1060.269 | 1061.677 |
| [ubiquitin + 3H] ³⁺ | 2855.970 | 12263.785 | 2858.252 | 2854.714 |
| [cyt- <i>c</i> + 3H] ³⁺ | 4121.050 | 14726.616 | 4124.269 | 4118.804 |
| [ubiquitin + 2H] ²⁺ | 4283.450 | 15013.956 | 4287.026 | 4281.392 |
| [cyt- <i>c</i> + 2H] ²⁺ | 6181.080 | 18029.799 | 6185.013 | 6178.576 |
| [ubiquitin + H] ⁺ | 8565.880 | 21218.503 | 8568.596 | 8563.868 |
| [cyt- <i>c</i> + H] ⁺ | 12361.150 | 25480.581 | 12359.345 | 12362.664 |

^a Boldface values are calibration points.

singly charged bradykinin, ubiquitin, and cytochrome *c* peaks were used to calibrate the spectrum, while the masses of multiply charged ubiquitin and cytochrome *c* were determined and compared with their known values. Results are presented in Table 5. For a two-term curve fit, the largest error was 3.92 Da. The RMS relative error was 677 ppm for this calibration. The error may seem rather high for a mass calibration, but it must be kept in mind that the masses are widely spaced. Excellent mass accuracy over such a wide range is not always realizable, particularly with a minimal number of calibrants and terms. Simplex yields similar results. For simplex optimization, we used the measured instrument parameters (listed in Table 4) and selected some parameters to optimize. We optimized the initial velocity of the ions and the error in locating the starting position of the time-of-flight mass spectrum. The optimized initial velocity is 350 m/s for these samples, and the start time average error is 17 ns. As displayed in Table 5, the largest error is 2.48 Da using these parameters. The RMS relative error for simplex was 410 ppm. This result is slightly better, though comparable, to the curve-fit calibration.

If simplex optimization accurately models ion flight for a broad range of extrapolated masses, then an otherwise difficult calibration might be possible with the simplex method. Such an example is the calibration of protein mass spectra using matrix peaks. To investigate this, we recorded mass spectra of bradykinin, ubiquitin, and cytochrome *c* using α -CHC as the matrix. This yielded 14 peaks between the masses of 146 and 12361 Da. First we examined curve fitting using two to seven matrix peaks and various numbers of terms in the fit equation. Table 6a summarizes our curve-fit results. The known masses and experimental times-of-flight are listed in columns 2 and 3 of this table. The subsequent columns list the errors in the fit. Boldface values in these columns represent the points used in the calibration. The remaining points are the data that were extrapolated from these fits. Using two terms and four calibrants, the mass of cytochrome *c* (12361 Da) was in error by 131 Da. Using two calibrants, this error was 975 Da. One may observe that the calibration points do not show any error in the two-term case. The fit minimized the error in the calibration points at the expense of mass accuracy outside the calibration range. With more calibrants and more terms, the matrix peaks were calibrated with very little error but the protein mass range greatly suffered. This can be seen in Table 6a for the five-term calibration with seven points, where the error was almost 6 MDa for the cytochrome *c* peak!

The curve-fit results reflect the difficulty in accurately calibrating protein peaks using matrix ions. We examined the accuracy

of simplex optimization by optimizing the flight tube length to see if this method could perform as well as or better than curve fitting. A summary of these calibrations is listed in Table 6b. The format of Table 6b is similar to that of Table 6a, in that boldfaced values represent the calibration points. Using two calibration points, the error in the mass of cytochrome *c* was about 9 Da. As we increased the number of calibration points, this error decreased and then increased. The worst accuracy for cytochrome *c* was observed with seven calibration points. Nevertheless, the error was only 12 Da. Furthermore, the errors for all of the other protein peaks steadily decreased as more calibrants were added. If one looks at the final columns of Table 6a,b, one may see a clear trend. Curve fitting was superior to simplex optimization in the calibrant region but was far inferior for extrapolated data. RMS errors are summarized in Table 6c. One may observe that as the number of calibrants increased, the calibrant error decreased for both curve fitting and simplex optimization. With extrapolated data, however, increasing the number of calibrants greatly increased curve-fit errors, while simplex accuracy actually improved. The poor (parts per thousand (ppt)) results even for the best calibrations require some qualification. First, with a mass of 100 Da, 0.1 Da error represents 1 ppt. Second, MALDI instruments are usually optimized to focus a narrow mass range and the matrix peaks are broader than they would be if they were the subject of greatest interest. Finally, the desorption velocities of MALDI matrix ions have been reported to be larger than those of protein ions.¹¹ This should make it more difficult to calibrate protein mass spectra using matrix peaks. This undoubtedly affects the accuracy of these calibrations. The desorption velocities of matrix ions have been reported to be higher than those of analyte ions.¹¹ Nevertheless, these results do show that simplex optimization can be used to provide calibration in a case where curve fitting cannot.

A 10-mer deoxyribonucleic acid (DNA) sample demonstrates the effectiveness of simplex optimization for calibration of a very broad range of masses with a minimal set of closely spaced calibrants. We chose as calibrants the (M - H)⁻ analyte peak and the (M + K - 2H)⁻ adduct peak and then determined the masses of some of the matrix peaks in the spectrum. These masses are listed in Table 7 with their corresponding measured flight times. A two-term curve fit yielded a mass for the first peak of 76.01 Da. With simplex optimization, the mass of this matrix peak was found to be 138.05 Da. Its actual mass is 138.11 Da, and the simplex algorithm makes it quite easy to correctly identify this peak in the congested matrix region of the spectrum. Four peaks displayed in Figure 5 are listed in Table 7. Clearly, simplex optimization allows correct identification of these peaks, while

Table 6. Calibration Error Summaries for Protein Spectra Using Matrix Peaks as Calibrants^a

| (a) Errors Using Curve-Fit Calibration | | | | | | | |
|--|------------------|----------------|--|------------------|------------------|------------------|------------------|
| identity | known mass (amu) | measd TOF (ns) | error (amu) vs numbers of terms and calibrants | | | | |
| | | | 2 terms 2 pts | 2 terms 4 pts | 3 terms 5 pts | 4 terms 6 pts | 5 terms 7 pts |
| [CHC – CO ₂ + H] ⁺ | 146.169 | 2786.656 | 0.000 | –0.289 | –0.140 | –0.106 | –0.084 |
| [CHC – CN] ⁺ | 164.162 | 2945.246 | 0.000 | 0.361 | 0.291 | 0.260 | 0.234 |
| [CHC – OH] ⁺ | 172.164 | 3017.444 | –0.535 | 0.147 | 0.033 | 0.005 | –0.014 |
| [CHC + H] ⁺ | 190.180 | 3172.972 | –1.645 | –0.221 | –0.288 | –0.279 | –0.266 |
| [CHC + Na] ⁺ | 212.162 | 3348.790 | –2.493 | –0.144 | 0.103 | 0.121 | 0.135 |
| [(CHC) ₂ – CO ₂ + H] ⁺ | 335.341 | 4208.657 | –9.455 | –1.272 | 5.974 | –0.002 | –0.009 |
| [(CHC) ₂ + H] ⁺ | 379.352 | 4475.787 | –12.123 | –1.685 | 10.122 | –2.571 | 0.004 |
| [bradykinin + H] ⁺ | 1061.180 | 7483.074 | –60.193 | –9.896 | 187.385 | –586.338 | 1380.472 |
| [ubiquitin + 3H] ³⁺ | 2855.970 | 12263.785 | –198.563 | –30.170 | 1382.069 | –10648.43 | 65714.9 |
| [cyt- <i>c</i> + 3H] ³⁺ | 4121.050 | 14726.616 | –299.699 | –44.214 | 2686.601 | –27075.23 | 220582 |
| [ubiquitin + 2H] ²⁺ | 4283.450 | 15013.956 | –313.066 | –46.291 | 2877.240 | –29797.41 | 249633 |
| [cyt- <i>c</i> + 2H] ²⁺ | 6181.080 | 18029.799 | –467.331 | –67.108 | 5448.326 | –72294.74 | 780900 |
| [ubiquitin + H] ⁺ | 8565.880 | 21218.503 | –662.705 | –92.301 | 9470.893 | –154873.3 | 2070261 |
| [cyt- <i>c</i> + H] ⁺ | 12361.150 | 25480.581 | –975.300 | –130.750 | 17398.76 | –356286.8 | 5985534 |
| (b) Errors Using Simplex Optimization | | | | | | | |
| identity | known mass (amu) | measd TOF (ns) | error (amu) vs number of calibration points | | | | |
| | | | 2 pts | 4 pts | 5 pts | 6 pts | 7 pts |
| [CHC – CO ₂ + H] ⁺ | 146.169 | 2786.656 | –0.414 | –0.500 | –0.553 | –0.616 | –0.660 |
| [CHC – CN] ⁺ | 164.162 | 2945.246 | 0.413 | 0.315 | 0.257 | 0.186 | 0.137 |
| [CHC – OH] ⁺ | 172.164 | 3017.444 | 0.284 | 0.182 | 0.121 | 0.047 | –0.005 |
| [CHC + H] ⁺ | 190.180 | 3172.972 | 0.116 | 0.003 | –0.064 | –0.147 | –0.204 |
| [CHC + Na] ⁺ | 212.162 | 3348.790 | 0.439 | 0.314 | 0.238 | 0.147 | 0.083 |
| [(CHC) ₂ – CO ₂ + H] ⁺ | 335.341 | 4208.657 | 0.841 | 0.643 | 0.524 | 0.379 | 0.278 |
| [(CHC) ₂ + H] ⁺ | 379.352 | 4475.787 | 1.010 | 0.786 | 0.651 | 0.487 | 0.373 |
| [bradykinin + H] ⁺ | 1061.180 | 7483.074 | 2.599 | 1.970 | 1.594 | 1.134 | 0.814 |
| [ubiquitin + 3H] ³⁺ | 2855.970 | 12263.785 | 8.217 | 6.522 | 5.508 | 4.269 | 3.408 |
| [cyt- <i>c</i> + 3H] ³⁺ | 4121.050 | 14726.616 | 11.20 | 8.753 | 7.288 | 5.499 | 4.255 |
| [ubiquitin + 2H] ²⁺ | 4283.450 | 15013.956 | 11.23 | 8.686 | 7.163 | 5.303 | 4.010 |
| [cyt- <i>c</i> + 2H] ²⁺ | 6181.080 | 18029.799 | 13.63 | 9.950 | 7.749 | 5.060 | 3.192 |
| [ubiquitin + H] ⁺ | 8565.880 | 21218.503 | 14.15 | 9.050 | 5.995 | 2.263 | –0.331 |
| [cyt- <i>c</i> + H] ⁺ | 12361.150 | 25480.581 | 9.289 | 1.905 | –2.515 | –7.913 | –11.67 |
| (c) RMS Error Summaries for both Calibration Methods (in parts per thousand) | | | | | | | |
| | | | number of calibrants | | | | |
| | | | 2 | 4 | 5 | 6 | 7 |
| RMS calibrant error for curve fit | | | 0.000 | 1.645 | 1.151 | 0.959 | 0.822 |
| RMS calibrant error for SO | | | 2.676 | 2.033 | 1.930 | 1.892 | 1.854 |
| RMS extrapolation error for curve fit | | | 56.769 | 9.005 | 754.48 | 13229 | 212346 |
| RMS extrapolation error for SO | | | 2.188 | 1.765 | 1.468 | 1.089 | 0.855 |

^a Boldface values are errors in the calibration points.

Table 7. Summary of Curve-Fit and Simplex Calibrations Using DNA Peaks and Adducts as Calibrants

| peak | | identity | | fit results | |
|-------------|-----------|--|------------|---------------|---------------|
| no. | TOF (ns) | moiety | mass (amu) | CF mass (amu) | SO mass (amu) |
| 1 | 2842.121 | [(3-HPA) – H] [–] | 138.110 | 76.010 | 138.046 |
| 2 | 3322.165 | [citrate – H] [–] | 191.117 | 130.495 | 191.071 |
| 3 | 3660.044 | [(3-HPA) ₂ – (CO ₂)] [–] | 232.196 | 172.510 | 231.978 |
| 4 | 3998.944 | [(3-HPA) ₂ – H] [–] | 277.213 | 218.710 | 276.970 |
| calibrant 1 | 13180.627 | [M – H] [–] | 3027.196 | 3027.196 | 3027.517 |
| calibrant 2 | 13262.534 | [M + K – 2H] [–] | 3065.287 | 3065.287 | 3065.430 |

curve fitting does not. Since extrapolation to lower masses is well-behaved, the masses between the matrix and parent ion regions could be determined with similar accuracy. This demonstrates a powerful ability of simplex optimization to calibrate an entire spectrum using a parent ion and an adduct peak. This calibration displays sufficient accuracy to identify all fragment or digest peaks

in a spectrum. Once a general set of parameters is determined, it is even possible to accurately calibrate a spectrum with only one calibration point. Typically, optimizing one parameter (such as V_{\max}) is sufficient for such a single-point calibration. This could be used to account for spot-to-spot mass spectral shifts commonly seen in MALDI-TOF experiments.

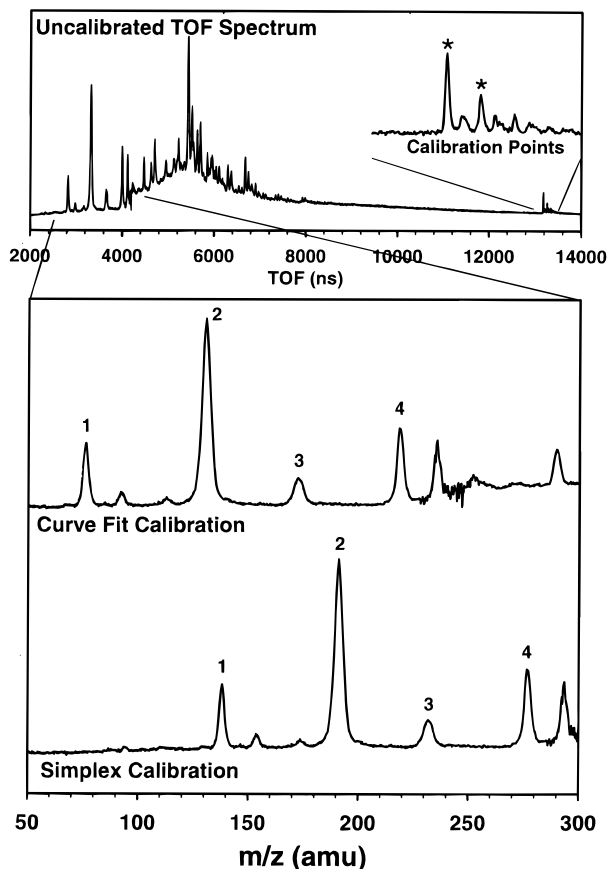


Figure 5. Uncalibrated time-of-flight spectrum of a DNA sample (upper) showing the chosen calibration points. The expanded matrix region is shown in the lower part of the figure after applying the two calibration methods. The simplex calibration allows for the accurate identification of these matrix peaks and performs well for the entire mass range of the time-of-flight spectrum. The curve-fit calibration leads to errors in this low-mass region.

When calibrants are chosen over a narrow and well-focused mass range, simplex optimization not only displays excellent performance but also can be used to extract information about the desorption phenomenon. A gold nanoparticle sample generated using direct laser desorption/ionization yielded a spectrum with a large number of narrowly spaced peaks. The known masses and times-of-flight of a sample are listed in Table 8, and Figure 6 is the TOF spectrum of this sample. The average desorption velocity of these ions is known to be different from that of a MALDI sample.²⁴ As discussed in previous work, the task of assigning these peaks was complicated by these differing desorption velocities, since MALDI-generated ions were used for the mass calibration. Using simplex optimization, we can examine the effect of desorption velocity on calibration and estimate the average desorption velocity for the gold sample. This also provides another example of the relative performance of curve fitting and simplex optimization for mass calibration.

For discussion of these calibrations, the RMS relative error was calculated from the equation

$$\text{error (ppm)} = (1 \times 10^6) \left[\frac{\sum \left(\frac{m_{\text{actual}} - m_{\text{calcd}}}{m_{\text{actual}}} \right)^2}{n} \right]^{1/2} \quad (7)$$

Table 8. Gold Nanoparticle Known Mass/TOF Pairs

| peak no. | mass (Da) | TOF (μ s) | peak no. | mass (Da) | TOF (μ s) |
|----------|------------|----------------|----------|------------|----------------|
| 1 | 12 683.748 | 23.470 138 | 16 | 13 567.808 | 24.273 812 |
| 2 | 12 715.812 | 23.499 807 | 17 | 13 668.583 | 24.363 694 |
| 3 | 12 880.715 | 23.651 423 | 18 | 13 700.647 | 24.392 039 |
| 4 | 12 912.779 | 23.681 212 | 19 | 13 732.711 | 24.420 182 |
| 5 | 12 944.843 | 23.710 098 | 20 | 13 764.775 | 24.448 866 |
| 6 | 13 045.618 | 23.802 025 | 21 | 13 865.550 | 24.538 166 |
| 7 | 13 077.682 | 23.831 180 | 22 | 13 897.614 | 24.566 233 |
| 8 | 13 109.746 | 23.860 600 | 23 | 13 929.678 | 24.594 347 |
| 9 | 13 141.810 | 23.889 813 | 24 | 13 961.742 | 24.622 739 |
| 10 | 13 274.649 | 24.009 884 | 25 | 14 094.581 | 24.739 942 |
| 11 | 13 306.713 | 24.038 739 | 26 | 14 126.645 | 24.767 729 |
| 12 | 13 338.777 | 24.067 933 | 27 | 14 158.709 | 24.795 736 |
| 13 | 13 471.616 | 24.187 472 | 28 | 14 323.612 | 24.939 527 |
| 14 | 13 503.680 | 24.215 949 | 29 | 14 355.676 | 24.967 084 |
| 15 | 13 535.744 | 24.244 621 | | | |

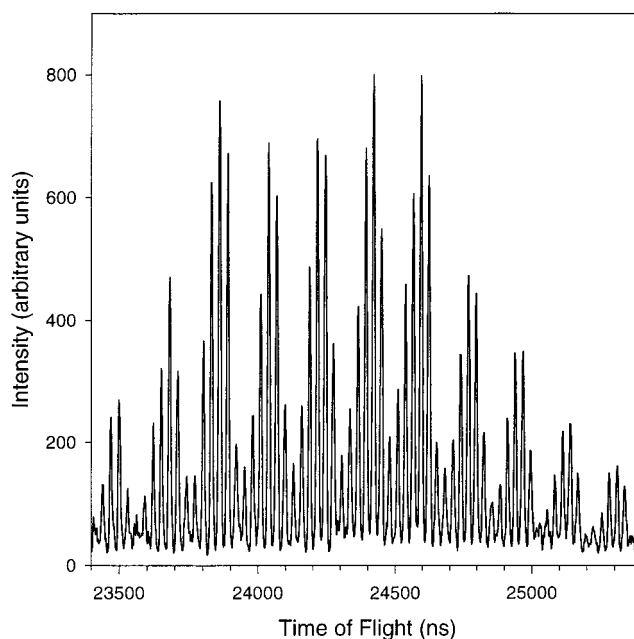


Figure 6. Time-of-flight mass spectrum of a gold nanoparticle sample.

Use of peaks 1, 4, 14, 26, and 28 listed in Table 8 gave a five-term curve fit with an RMS relative error of 23.387 ppm. Measured parameters for the instrument are specified in Table 4, and these were entered into the simplex routine. Interestingly, simplex optimization could not converge on reasonable values when a 600 m/s desorption velocity was used independent of the number of instrument parameters varied. A rapid trial and error analysis showed that an initial velocity of 100–200 m/s did lead to convergence. Optimization of four selected parameters using an initial velocity of 100 m/s gave a voltage pulse of -5418.16 V, a flight tube length of 0.322221 m, a τ value of 3.19628 μ s, and a start-time error of -0.584 ns. This yielded an RMS relative error of 3.306 ppm for all 29 points. Optimizing the initial velocity parameter gave a desorption velocity of 72.179 m/s, a flight tube length of 0.32341 m, and a start-time error of 4.71820 ns, yielding a similar accuracy. Because we did not measure the desorption velocity of this sample, we arbitrarily used 100 m/s for the remainder of this analysis. If the calibrants are moved inward (using points 4, 7, 11, 17, and 23), the RMS relative error for the

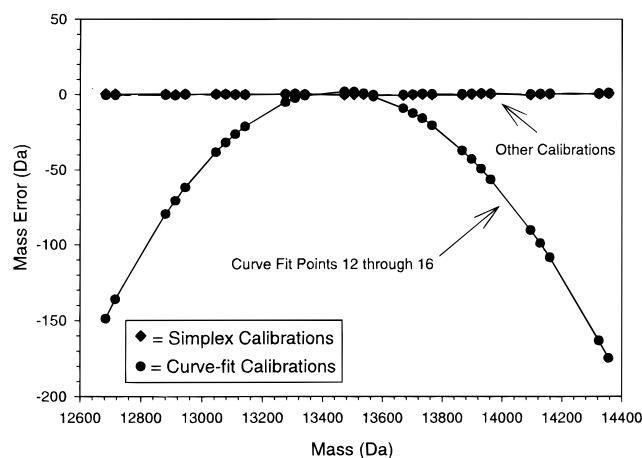


Figure 7. Residual errors of calibrations of the gold nanoparticle sample using various calibration points, for both curve fitting and simplex optimization. (Simplex optimization allows for a calibration that is consistent regardless of the actual points chosen for calibration. Curve-fit calibrations are more susceptible to experimental errors that limit extrapolation accuracies.)

curve fit is 106.94 ppm. If the middle five points (12–16) are used, the error increases to 8727 ppm. In comparison, simplex optimization displays errors of 3.254 and 5.287 ppm in these cases, respectively. Figure 7 is a plot of the residual errors for each known mass using both methods with well-spaced (points 1, 4, 14, 26, and 28) and poorly spaced (points 12–16) calibrants. Immediately apparent in this figure is the significant error in the curve-fit calibration using poorly spaced calibrants. When the calibrants are distributed better, the errors are low throughout the calibration range. For simplex, on the other hand, the calibration appears to perform well regardless of the range of calibrants. In Figure 7, these results virtually overlap the best curve-fit calibration and are thus difficult to distinguish. Errors in the extrapolated data limited the overall accuracy of the curve fit. Simplex optimization, on the other hand, did not show these large deviations in the extrapolated regions. In experimental data, finite errors can arise from inaccuracies in determining peak positions. In our case, the limited number of points for each peak (about 7–10 points using a 2 ns/channel digitization rate) combined with deviations from Gaussian behavior limited the accuracy of measured data. Additionally, two Gaussian peaks that slightly overlap each other have their apparent locations shifted toward each other. Experimentally determined samples will always show some small but finite error. Simplex optimization calibration is less sensitive to these small random errors, which leads to an overall improvement in calibration performance. The extreme case of using points 12–16 for calibration provides another example of how curve fitting does not permit predictable and accurate extrapolation, while simplex optimization does. This is consistent with the DNA and protein/matrix calibrations discussed above.

Fortunately, mass spectra can usually be calibrated by using surrounding unknown peaks with a good set of calibrants. When points 1, 2, and 29 from Table 8 were used in a two-term curve-fit calibration, the RMS relative error of all points was 4.562 ppm. The low error for this two-term fit was due to a number of factors. First, a mass range where the smallest mass is close to the largest mass (a narrow mass range) has a lower dependence on higher order nonlinearities and a two-term calibration sufficiently models

this. Second, the calibrants encompass the entire mass range and the number of calibrants exceeds the number of terms in the equation (the system was overdetermined). Simplex calibration shows a similar quality fit using these calibrants, and optimizing four parameters results in an error of 4.206 ppm. In general, we find that simplex optimization and curve fitting are comparable for interpolated masses. Of course, an advantage to the simplex method is that unknown parameters such as desorption velocity can be estimated. Finally, the mass accuracies of these measurements were in the parts per million range, which demonstrates that a narrow mass range will display better mass accuracy than a broad range. Because the masses of the gold nanoparticles were confined to a narrow range, our calibration accuracies were in the realm commonly reported for mass calibrations.

Caveats Regarding Simplex Optimization. Because this work has demonstrated a number of advantages of the simplex approach to mass calibration, it is appropriate to consider practical aspects involved in using this method. First, instrument conditions must be measured. In contrast, curve fitting does not require knowledge of instrument parameters. Laboratory measurements may not yield accurate values for these parameters. For example, regardless of the accuracy with which a distance between two grids is measured, a field that penetrates through a grid will change the dimension of a field in this region. Because of such measurement difficulties, the parameters to simplex-optimize should be carefully chosen. The optimization can correct for errors in measurement, so if the parameters to optimize are those with the largest uncertainties, the simplex procedure will compensate for measurement errors. In some cases, despite the best efforts, the optimized parameters may deviate from physically realistic values. As illustrated for theoretical data, such unrealistic parameter values can be due to errors in calibration points that lead to mediocre, but usable, calibrations. Therefore, values of instrument parameters should be constrained within reasonable limits in optimization calculations. Apparently unrelated parameters can be intimately coupled. For example, the ion velocity at the time of extraction depends on whether the field in the source region prior to extraction is exactly zero. Initial-velocity determinations may even be complicated in that different masses may have different velocities.¹¹ Investigations of this may lead to calibration improvements if the desorption velocity is introduced as a mass-dependent function. It might seem that the simplex optimization mass calibration routine would be slower than curve fitting because it is accounting for so many instrument parameters. This is not the case, as the routines are very fast. On a personal computer, both simplex optimization and curve fitting have essentially equal performance, and both appear to be essentially instantaneous to a user.

SUMMARY AND CONCLUSIONS

By comparisons of the curve-fitting and simplex optimization approaches to TOF mass calibration, some of the advantages of the latter method have become apparent. First, it was shown that simplex optimization is relatively immune to improperly assigned calibrants. This is important when mass calibrants have errors due to unexpected modifications or limited instrument accuracy. Second, it was shown that the number of parameters that can be optimized is not constrained by the number of calibrants and an underdetermined system may still be calibrated. Third, although

the methods are comparable when calibration peaks surround the unknown analyte, the simplex approach is far superior for extrapolating a calibration curve beyond the mass range of known calibrants. This was demonstrated by calibrating an entire spectrum using a single DNA peak and its adduct and by using only matrix peaks for a protein calibration. Fourth, it may be possible to estimate parameters such as ion desorption velocity that may vary from sample to sample.

Although the general approach was demonstrated for a linear TOF system, this method should work equally well for any TOF geometry. For example, a collection of spectra with varying reflectron voltages is often recorded in postsource decay experiments. Since only one instrument parameter is varied in these experiments, simplex optimization may prove to be useful for

calibration of these spectra. In general, we have found this algorithm to be fast, robust, and well suited to a wide variety of calibrations.

ACKNOWLEDGMENT

We acknowledge the National Science Foundation for supporting this work, and N.P.C. thanks the Indiana University College of Arts and Sciences for a Cooperative Graduate/Undergraduate fellowship.

Received for review December 30, 1999. Accepted March 29, 2000.

AC991500H